

Hydrodynamic interactions in deep bed filtration

Claude Ghidaglia

Laboratoire de Physique et Mécanique des Milieux Hétérogènes, URA 857 au CNRS, ESPCI, 10 rue Vauquelin, 75231 Paris Cedex 05, France

Lucilla de Arcangelis

Laboratoire de Physique et Mécanique des Milieux Hétérogènes, URA 857 au CNRS, ESPCI, 10 rue Vauquelin, 75231 Paris Cedex 05, France and Dipartimento di Fisica, Università dell'Aquila, via Vetoio, 67010 Coppito L'Aquila, Italia

John Hinch

Department of Applied Mathematics and Theoretical Physics, University of Cambridge, Silver Street, Cambridge, CB3 9EW, United Kingdom

Elisabeth Guazzelli

Laboratoire de Physique et Mécanique des Milieux Hétérogènes, URA 857 au CNRS, ESPCI, 10 rue Vauquelin, 75231 Paris Cedex 05, France

(Received 15 May 1995; accepted 7 September 1995)

Deep bed filtration has been studied experimentally and numerically for small non-Brownian particles flowing into a random packing of monosize glass spheres at low Reynolds number. It was discovered that packets of particles penetrated further than the same number of particles released one at a time. These collective effects are attributed to hydrodynamic phenomena, one plausible explanation being the existence of relaunchable “hydrodynamic captures” in addition to “geometric captures.” © 1996 American Institute of Physics. [S1070-6631(96)00701-5]

I. INTRODUCTION

Deep bed filtration is a long-established engineering process in which small suspended particles in a fluid deposit at various depths within the pores of a bed of granular material (see, for instance, the full-length survey by Tien¹ and the more focused reviews by Herzig *et al.*,² Tien and Payatakes,³ Dodds *et al.*,⁴ and Houi⁵). It is generally used to clarify dilute suspensions of small particles (less than 10 μm) in low concentrations (less than 5×10^{-4} g/cm³). The flow rate of the suspension in the filter is in the order of one mm/s, and cleaning may be achieved by simply reversing the direction of the flow.

During the filtration process, the transportation and capture of the solid particles in the filtering medium are due to several forces and interactions. The relative importance of these forces is determined by the size of the particle. When the diameter of the suspended particles is larger than 10 μm , the dominant forces are the hydrodynamic and gravitational forces, i.e., the drag force, the lubrication force, the gravitational force, and the inertial force. When the particles are smaller, the electrochemical forces such as the Van der Waals and double-layer forces and the Brownian diffusion dominate. Six common capture mechanisms are found in the literature.¹ One of the major mechanisms for aerosol collection for particles with diameter larger than 1 μm and in the absence of applied external forces is inertial impaction. Particle deposition by interception can occur because the particles are finite in size, while deposition by sedimentation occurs when the particle density is different from that of the fluid. Electrostatic forces and Brownian diffusion can also be

important factors for small particles. A final mechanism, which plays a dominant role in our experiments, is known as straining or sieving and is due to a steric effect. It arises when the particles are retained in the pore constriction of the granular media. In most situations of practical importance, a number of these mechanisms are operating simultaneously.

Deep bed filtration is inherently an unsteady-state process because the pore space is continuously modified by the motion and deposition of the small particles and thereby the flow pattern is continuously changing. In most of the experimental studies,¹ the process evolution has been followed by measuring the pressure drop between the entrance and the end of the filter (or the permeability of the filter) and the efficiency of the filter (the ratio between the influent and effluent particle concentration). Visualization experiments have also provided information regarding particle deposition^{5,6} and the influence of the filter structure on the flow pattern.⁷

Deep bed filtration has been modeled as a deterministic process.¹ Macroscopic equations based on the conservation principle are then solved by assuming particular laws for the filtration rate. It has been also described as a stochastic process.¹ It is then necessary to define a set of random variables describing the empirical process whose evolution is governed by probability laws. Four types of numerical models related to these approaches have been classified in the literature (see, for instance, the reviews by Herzig *et al.*,² Tien and Payatakes,³ and Sahimi *et al.*⁸). In empirical models, mass balance equations are solved without trying to make explicit the physics of the deposition processes. Em-

pirical correlations are used to describe rate laws for deposition and the evolution of the particle concentration. Although they are mathematically simple, the stochastic models too do not provide a precise description of the deposition mechanism. They do not consider the effects of pore size and particle size distribution, or the deposition morphologies, on the filtration processes. Trajectory analysis models represent the filter as unit bed collectors. The trajectory of each particle within the unit bed is calculated using streamline functions combined with the forces acting on the particles. While these approaches have been fairly successful in describing the phenomenon at the pore size, they fail to predict the permeability change during the filtration process. In network models,⁹ the pore space is modeled as a network of tubes and the particle propagation is essentially governed by the flow field. Network models can account for the effect of pore space morphology in a realistic manner and therefore seem to be most successful in providing fundamental insight into the filtration process.⁸⁻¹²

The present work concerns the deep bed filtration of non-Brownian particles carried inside a model porous medium under laminar flow conditions. The porous medium consisted of a random packing of monosize glass spheres. Small marked particles were tracked inside the packing made optically transparent by matching the index of refraction of the fluid to that of the glass spheres of the packing.¹³ The objective of this study is to characterize the particle penetration depths by considering only the hydrodynamic and gravitational forces along with the important sieving from the geometric structure of the packing. We should emphasize here that in practical deep bed filters other mechanisms can also be important. The penetration depth distributions are examined for different particle injection methods, i.e., individually or in packets. A Monte Carlo simulation that approximated the packing by a two-dimensional square network of cylindrical tubes was developed jointly with the experimental study. Direct comparison with experiments allows one to test the validity of the various basic ingredients introduced in the numerical model. The problem of the particle capture transition is examined in another study.¹⁴

The present paper is organized as follows. The experimental techniques are presented in Sec. II. Experimental observations and statistical analyses of the particle penetration depths are described in Sec. III. The numerical model is introduced in Sec. IV. In Sec. V, the predictions of the model are compared to the experimental observations and the ingredients of the model are discussed. Conclusions are given in Sec. VI.

II. EXPERIMENTAL TECHNIQUES

A. Filter, particles, and fluid

The conceptually simple experimental model used to study deep bed filtration is based on a visual observation of small marked particles in a random fixed bed of larger glass spheres, made optically transparent by matching the refractive index of the suspending fluid to that of the larger glass spheres.

The filter consisted of a fixed random packing of glass

spheres of equal size and density. Two batches of glass beads were used with diameters $D_1=4.0\pm 0.1$ mm and $D_2=5.0\pm 0.1$ mm. The first layer of the packing was partially filled with larger glass spheres of diameter 10.0 ± 0.1 mm, which induced a roughness at the entrance of the bed. This local roughness induced disorder throughout the bed and avoided the formation of a crystalline zone that would alter the random structure of the packing.¹⁵ A uniform porosity of 0.39 ± 0.01 was measured along the cell. This showed the homogeneity of the packing. This measured porosity is equal to that of a random packing of spheres.

The small particles to be filtered were made from acrylic resin with a density $\rho_p=1.19\pm 0.01$ g/cm³. These particles were coated with a uniformly smooth thin layer of gold using a metal deposition device (Polaron High Resolution Sputter Coater E5400) so they could be clearly tracked in the filter. The thin coating has inconsequential effects on the particle weight. The particle size distribution was analyzed using a digital imaging system. From the measurements of the projected particle surfaces, the particle diameter distribution was found to be approximately Gaussian and the mean diameter and standard deviation were determined. Two batches of marked beads were used. The first batch had a diameter $d_1=650\pm 40$ μ m and the second a diameter $d_2=830\pm 30$ μ m. The error in the diameter of the small particles is one standard deviation of the size distribution.

Two combinations of particles and glass spheres were chosen to study the particle capture inside the random packing. In the first combination, the particles of diameter d_1 were injected into the random packing of glass beads with diameter D_1 . This combination corresponds to a value of the ratio between the small particle diameter and the large sphere diameter $\theta_1=d_1/D_1=0.162\pm 0.009$. The second combination corresponded to particles with diameter d_2 and glass spheres with diameter D_2 , i.e., a value $\theta_2=0.166\pm 0.007$, close to the value of θ_1 . In both combinations, the dimensionless parameter $\theta=d/D$ is larger than the capture threshold value, and thereby the particles were always captured inside the filter. The error in θ is based on consideration of the errors in the diameters d and D of the particles and the packing spheres, respectively.

The carrier fluid was an organic mixture of 60% dibutyl phthalate and 40% butyl benzyl phthalate (Santizer 160 produced by Monsanto) with a density $\rho_f=1.07\pm 0.05$ g/cm³, a kinematic viscosity $\nu=29\pm 1$ cS and a refractive index of 1.520 ± 0.005 , equal to that of the large glass spheres at 25 °C. The fluid viscosity was measured with a viscosimeter and its Newtonian behavior was also checked. This fluid dissolves plastics, which led to the choice of resistant materials such as stainless steel, glass, and teflon in the construction of the cell (see the following section).

B. Experimental procedure

Experiments were performed in a cell of rectangular cross section with an inside width of 125 mm, an inside depth of 39 mm, and a height of 430 mm. A few earlier experiments were also carried out in another cell having inner dimensions of 100 mm by 39 mm by 550 mm. The width

and depth of the vessel were uniform to within 0.05 cm. The restriction on the depth of both cells comes from the difficulty of seeing a long way inside the filter, despite the good index matching. The front and back of both cells were made of glass to allow visualization. The fluid was usually circulated upward through the cell. A few experiments were also undertaken using a downward flow circulation. At the entrance of the cell, the flow was made laminar by using different layers of porous materials. The flow rate was maintained constant by means of a pump and the interstitial velocity was $U = 0.43 \pm 0.01$ cm/s. The Reynolds numbers based on the length scale of the particles or that of the glass spheres were then always kept at a value smaller than unity. The particles Brownian Péclet number was always very large.

The random packing was maintained by two grids inside the cells. The small particles were injected with a syringe into a layer of fluid of 50 mm below the packing and then carried by the flow into the packing. Two kinds of particle injection were used. In the first, the particles were injected one by one. Each particle was injected as soon as the preceding particle was captured or left the filter and therefore propagated alone in the filter. There was no interparticle interaction in this type of injection. Conversely, in the second kind of injection, the particles were injected in packets. This type of injection was much trickier to perform since it was difficult to inject the packets in such a way that all the particles would flow into the packing at the same time. There was a spread of the order of 1–3 s between the entrance of the different particles into the packing. It should also be mentioned that the particles never came into very close contact and were never found to aggregate as they propagated inside the filter. In both injections, the particles remained inside the packing after capture. It should be noted that it seldom occurred that two particles were captured in the same site.

The cell was lit from behind and the particles were then easily tracked inside the packing. The initial position of a particle as it entered the packing and the final position when it was captured were recorded. Only the final capture positions were recorded when the particles were injected by packets. The precision of the measurement of the position was limited by parallax errors of the order of a millimeter caused by the thickness of the cell wall and variations in the glass sphere indices. The penetration depth was defined as the difference between the initial and final vertical coordinates, ΔZ , and the lateral dispersion as the difference between the initial and final horizontal coordinates, ΔX . From these measurements, the particle penetration depth distribution was determined. In the case of the one by one injection, it was also possible to measure the particle lateral dispersion distribution. Particles flowing along the cell walls were not taken into account in the statistical results because the pore sizes along the wall were much larger than those inside the packing. A number of 200 particles was injected for each experiment to give good statistics. Dismantling the experiment involved cleaning the cell, filtering the fluid, and washing and drying the glass spheres, in preparation for the next experiment.

III. EXPERIMENTAL RESULTS

A. Particle propagation

When the particles were injected one by one, their trajectories inside the filter were observed to be very straight. This finding was confirmed by measuring the particle lateral dispersion. The lateral dispersion distributions were found to be centered on the zero value and to be very narrow with a width smaller than a diameter of the large glass spheres. When the particles were injected by packets, the packet was also observed not to spread much along the cell width direction. These experimental findings suggest that the particles were convected inside the packing and that steric effects and hydrodynamic and gravity forces were dominant. Since the cell depth was of the order of ten glass sphere diameters, these findings also show that wall effects were negligible in these experiments.

B. Particle capture

One of the objectives of this work was to analyze the particle capture mechanism when steric effects and hydrodynamic and gravity forces were dominant. It is, however, important to estimate the influence of other forces, such as inertial, electrostatic, Brownian, and molecular forces in this process. Since the particle Reynolds number and also the Stokes number were small, the inertial force was negligible compared to the viscous forces and the particles followed the motion of the fluid. Electrostatic forces were also negligible in the experiments because the particles were gilded and the organic carrier fluid contained no charges. Brownian motion was also negligible compared to convective motion since the Brownian Péclet number was very large. The following considerations provide an estimate of the relative importance of the molecular forces. Since the sphere of the packing is greater than the particle, then the former can be approximated by a plane and the Van der Waals force can be expressed as $F_{\text{vdw}} = \pi H d^3 / [12 h^2 (d + h)^2]$, where H is the Hamaker constant ($\approx 10^{-19}$ J) and h is the distance between the particle and the large glass sphere. The gravity force is $F_g = \pi d^3 (\rho_p - \rho_f) g / 6$ and the drag force is $F_{\text{drag}} = 3 \pi \nu \rho_f U d$. It should be mentioned that the expressions for these forces do not take into account the direction of the forces that are, except for the gravity force, very difficult to determine. Taking the distance between the particle and the glass sphere to be 1 μm , which was typically the particle roughness as measured from photos obtained by electronic scanning microscopy, the gravity force was 8000 times the Van der Waals force and the drag force was 20 000 times the Van der Waals force. This calculation shows that when particles flowed inside the filter the Van der Waals force was negligible. Conversely, when the particles were captured, the distance between the particle and the glass sphere could become small enough to yield a Van der Waals force of the same order as the drag force (or the gravity force). This last effect is supported by the fact that captured particles were not observed to fall under gravity force when the upward flow was stopped.

The main capture mechanism was sieving due to the geometrical structure of the filter. Particles were indeed gen-

erally captured in constriction sites. However, the following discussion shows that additional capture sites were determined by the hydrodynamic and gravity forces at work inside the filtering medium. When a large sharp variation of the upward flow rate was induced (by hitting the pump), the flow remaining laminar, 15%–20% of the captured particles left the capture sites, propagated again in the medium until they were captured once again at other sites. These relaunching of particles were not observed when the flow rate was progressively increased, although probably to more modest levels. This “relaunching phenomenon” seems to be due to a sharp pressure variation inducing hydrodynamic forces large enough to dislodge the particles from their capture position. This experimental observation also seems to suggest that the lubrication forces did not have a significant action on the particle since these relaunchings occurred at time scales (of the order of one minute) much shorter than the time needed for two surfaces to come into close contact under lubrication forces. The surface roughness should also prevent the particles from getting very close to a sphere surface. The existence of this “relaunching” phenomenon shows the influence of flow variations on the stability of the capture sites and supports the existence of capture sites, which are partially hydrodynamic in nature. These sites could be, for example, stagnation points of the flow. A particle moving along the flow line near a collector could also be intercepted by the collector or could settle under gravity in a site, where it later became bonded by Van der Waals forces. The direction of the flow also had an influence on these relaunching. When the flow direction was downward (parallel to gravity), more than 50% of the particles were released under sudden flow rate variations. This new observation demonstrates that the gravity forces also played an important role in the particle capture mechanism and in the stability of the capture sites. Moreover, the measured capture threshold value, $\theta_c = 0.140 \pm 0.005$, was found¹⁴ to be slightly smaller than the geometric capture value, $\theta_g = 0.155 \pm 0.006$, corresponding to the smallest possible pore formed by three identical spheres in contact.¹⁶ This last finding also supports the existence of “hydrodynamic” sites. Finally, it was noticed that when packets of particles propagated inside the filter, a particle captured in a site could be relaunched by another particle passing nearby. This observation can be related to the relaunching phenomenon mentioned above. The local velocity variations induced by a moving particle could produce local “relaunching” of particle captured in a “hydrodynamic” site. In contrast, when the particles were injected one at a time, we tentatively suggest that the slower injection procedure allowed time for the particles in hydrodynamic capture sites to become bonded by Van der Waals forces so that they were not relaunched by later passing particles.

C. Penetration depth distributions in the case of an upward flow

Figure 1 shows the penetration depth distribution of 200 particles injected one by one in the case of an upward flow and for $\theta_1 = 0.162 \pm 0.009$. Since a simple probabilistic model without flow predicts an exponential decay of the histogram,^{13,17} the distribution was fitted to an exponential

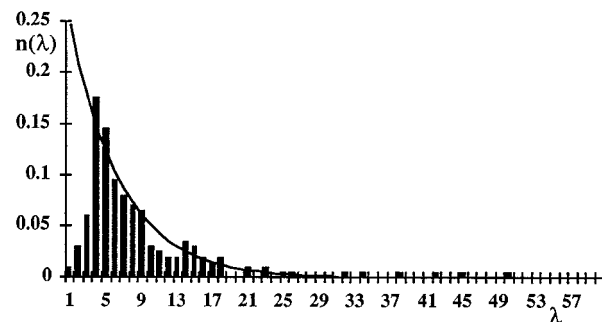


FIG. 1. Experimental results for the particle penetration depths for $\theta_1 = 0.162 \pm 0.009$ when particles were injected one by one with an upward flow.

decay law, $\exp(-\lambda/\xi)$ with $\lambda = \Delta Z/D$. Here and in the remainder of the paper, all the lengths have been made dimensionless by scaling with the diameter of the large glass spheres. This law did not fit the whole histogram. The first three bars were eliminated, as they correspond to particles captured at the entrance of the bed, where it is inhomogeneous due to the presence of a few larger spheres. In order to quantify the agreement with an exponential decay, the χ^2 test was used. The normalized indicator χ^2 , which measured the difference between the actual values and the exponential distribution, was found to be 0.91. Although the propagation laws and the capture mechanisms in the experiment were more complex than a simple probabilistic model, the validity of the exponential fit was then ensured. This test also provided a confidence interval for the characteristic length ξ . A confidence level of 10% was chosen. The exponential fit was judged reasonable if the value of χ^2 calculated is less than $\chi^2(10\%)$, knowing that 90 experiments out of 100 would give an acceptable answer if the exponential law was true. By varying the exponential decay coefficient, two values for which $\chi^2 = \chi^2(10\%)$ were obtained, which gave the confidence interval for ξ . The characteristic length was found to be $\xi = 5.5 \pm 0.9$. The mean penetration depth $\langle \lambda \rangle$ and the median value, λ_m , for which $\sum_{\lambda \leq \lambda_m} n(\lambda) = \frac{1}{2}$, where n is the number (normalized by the total number of injected particles) of particles captured at a depth λ were also measured. The reason for considering both the mean and median is to take into account particles that exit the bed, which is done with our definition of the median, whereas the mean is determined only for captured particles. In the present case, the mean penetration was $\langle \lambda \rangle = 8.4$ and the median value $\lambda_m = 6.0$. It is important to notice that the median value is close to the value of the decay length and provides a good characterization of the penetration depth of the particles inside the medium. For a given value of θ , the experiments were found to be perfectly reproducible.

Figure 2 displays the penetration depth distribution of 200 particles injected in three packets (each containing about 65 particles). In this case, the distribution is not at all exponential, as demonstrated by the χ^2 test, and presents a much slower decrease. In the previous case where particles propagate independently inside the filter, the penetration depth dis-

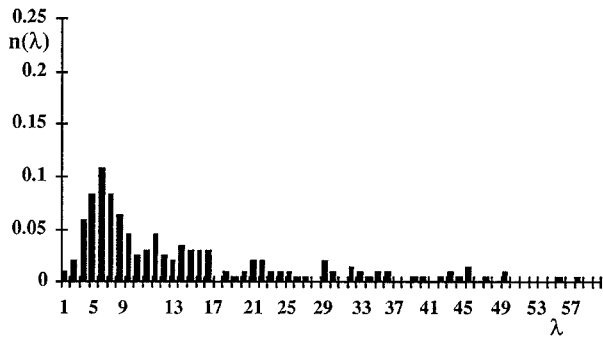


FIG. 2. Experimental results for the particle penetration depths for $\theta_1=0.162\pm 0.009$ when particles were injected by packets with an upward flow.

tribution presents a peak value of 0.17 and a very few particles penetrate farther than a distance of 20 beads (see Fig. 1). Conversely, when packets of particles propagate, the value of the peak is 0.11 and a significant number of particles reaches distances larger than 20 beads (see Fig. 2). In this later case, the median value, $\lambda_m=9.3$ is larger than that ($=6.0$) found in the case of the one by one injection. Therefore, packets of particles penetrated further than the same number of particles released one at a time. Although it was very difficult to control precisely the number of particles contained in a packet, the experiments were again found to be perfectly reproducible.

Finally, although the particles remained inside the filter after capture, their presence did not affect the penetration depth distribution. The number of captured particles was so small than they did not saturate the packing. Indeed, each of the 60 layers of the packing contained 250 pores, and only 200 moving particles were injected in the whole bed. Moreover, in the case of the one by one injection, the penetration depth distribution for the first 100 particles had the same behavior and statistical characteristics (mean and median values) as that obtained for the last 100 particles. In the case of the injection by packets, the penetration depth distributions corresponding to each packet were also similar. These last findings also confirm the absence of saturation of the filter.

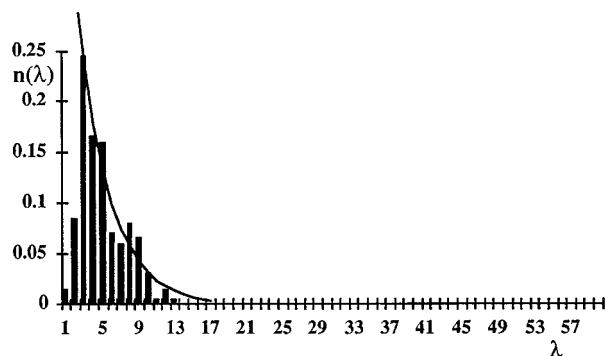


FIG. 3. Experimental results for the particle penetration depths for $\theta_1=0.162\pm 0.009$ when particles were injected one by one with no flow.

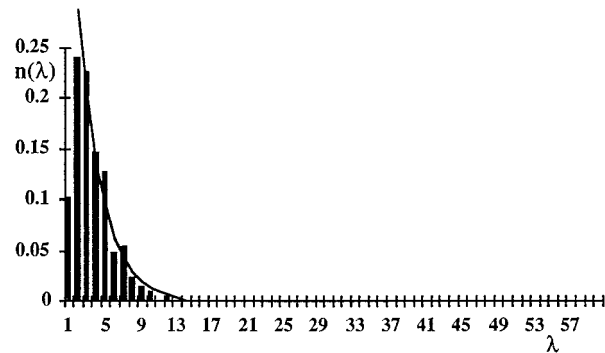


FIG. 4. Experimental results for the particle penetration depths for $\theta_1=0.162\pm 0.009$ when particles were injected by packets with no flow.

D. Penetration depth distributions in the case of no flow

Experiments were also performed without flow. The particles were dropped (from the top of the packing) into the filter and only propagated under gravity forces.

Figure 3 shows the penetration depth distribution of 200 particles injected one by one in the absence of flow. The distribution can be fitted with an exponential law, as demonstrated by the χ^2 test. The characteristic length of the exponential decay is $\xi=3.4\pm 0.6$ and the median value of the distribution is $\lambda_m=4.0$. In absence of flow the particles penetrated slightly less deep in the medium than in the case of particles convected by the flow (see Fig. 1). Clearly, the flow leads the particles toward the biggest pores and therefore the probability for a particle to be captured is lower when it is carried by the flow than when it just falls under gravity.

The penetration depth distribution of particles propagating by packets in the absence of flow has the same behavior as that of particles injected one at a time without flow, as displayed in Fig. 4. The distribution can be indeed fitted in both cases by an exponential law and the particles penetrated less deep into the packing when they are injected by packet without flow than when they are injected by packets with a flow. The characteristic length of the exponential decay is $\xi=2.6\pm 0.6$ and the median value of the distribution is $\lambda_m=2.8$. These values are much smaller than those found when packets of particles are flowing inside the filter.

These experiments show that the “packet effect,” i.e., the deeper penetration of packets of particles than that of same number of particles released one at a time, found when the particles are convected by an upward flow is not observed without flow. This finding suggests that the collective effect when the particles are injected by packets is due to hydrodynamic phenomena.

E. Penetration depth distributions in the case of a downward flow

A few experiments were also performed for particles propagating with a downward flow (in the same direction as that of the gravity force). In that case, the penetration depths were not easy to measure because relaunchings of particles were very frequent and thereby the capture positions were

TABLE I. Median values of the penetration depth distribution, λ_m . The values are made dimensionless by scaling with the diameter of the spheres of the packing.

Number of particles in a packet	1 ^a	10	20	35	50	65
$\theta_1=0.162 \pm 0.009$	6.0		10.0		11.5	9.3
$\theta_2=0.166 \pm 0.007$	3.6	5.0		5.6		

^aParticles injected one by one.

not found to be very stable (this phenomenon was also observed when particles were dropped inside the packing without flow). Therefore the penetration depth distribution was built from the recording of the first capture positions of the particles. The “packet effect” was still observable, but it was less perceptible than in the case of the upward flow, for which the capture positions were clearly determined. In the packet case with a downward flow, the penetration depth distribution could again not be fitted by an exponential law according to the χ^2 test, and the particles penetrated deeper into the packing than in the case of the one by one injection.

F. Effect of the number of particles in a packet

The influence of the number of particles in a packet was also examined. Experiments were undertaken where packets of a given number of particles were injected in an upward flow. The size of the packet was varied. It was not possible to inject packets of larger size because the packet did not keep together in the medium, and so it was equivalent to injecting a packet of smaller size. The relative error in the number of particles in a packet was 20%. For each experiment with packets of a given size, a total 200 particles were injected over several packets. Two close values of θ but with different values of d and D were examined, $\theta_1=0.162\pm 0.009$ and $\theta_2=0.166\pm 0.007$. In both cases, the particles penetrated deeper inside the filter when they were injected by packets than when they were injected one by one. However, the “packet effect” was not found to be very sensitive to the size of the packet. Indeed, the median value of the penetration depth distribution did not vary much with the size of the packet, as can be seen in Table I. It should also be noted that although the values of θ_1 and θ_2 are very close, the “packet effect” was found to be more pronounced in the first case where the injected particles were smaller. This finding suggests that the parameter θ may not be the only scaling parameter.

IV. NUMERICAL MODEL

A. Pore space

The porous medium was represented by a two-dimensional network⁹ of cylindrical tubes of given radius, r , and length, l . A tube was assumed to represent a pore of the filtering medium. The tubes intersected at points of mixing called nodes. Since a random packing has been usually represented as an ensemble of tetrahedral units with a connectivity of 4, a square network was chosen.^{18,19} It was checked by using a triangular network (with a connectivity of 6) that the connectivity was not a relevant parameter for the present

study. The network was inclined at an angle of 45° and its dimension was 40 wide by 120 in the direction of flow. The unit length was chosen to be the characteristic length of the experimental sphere packing, i.e., the diameter of the glass bead. Since constriction sites were found to determine primarily particle capture, the sizes of the tubes were determined by the sizes of the pore entrances instead of the sizes of the cavity volume. The distribution of the tube radii was chosen to be a power law, $(r-\theta_g)^{-0.5}$, with a cutoff at the geometric threshold value θ_g , as suggested by the numerical results of Mason.¹⁸ The cylinder length was made proportional to the pore radius since a correlation was expected between the width and the length of the pores.

B. Fluid velocity field

The flow rate, Q , of the viscous fluid was supposed to obey Poiseuille’s law in each tube, $Q=\pi r^4 \Delta P_p/8l\nu\rho_f$, where ΔP_p was the pressure drop along the tube. A perfect mixing was also assumed at each node. The fluid velocity in each tube was calculated as the mean velocity, $Q/\pi r^2$. The fluid-flow problem was then analogous to current flow in a network of random resistors, whose conductance was expressed in terms of the radius and length of the tube and Ohm’s law could be substituted for Poiseuille’s law. Since in the experiments the flow rate was maintained constant, the current between the top and the bottom of the network was also maintained constant. Periodic boundary conditions were imposed in the other direction. Mass balance equations for the fluid need to be solved simultaneously at each node. This was done by solving a standard Kirchoff’s law formulation. Both conjugate gradient and numerical relaxation methods were used. After convergence (with a 10^{-10} accuracy), the pressures at each node were calculated. Once the flow field within the network was determined, particles, which were supposed to be spherical and whose radii were selected from the experimental particle size distribution, were injected into the network.

C. Particle propagation mode and capture mechanisms

1. Particle propagating alone in the network

A single particle was injected into the network on the upstream plane of the network. An inlet tube among the 80 available tubes in the 40 by 120 network was selected. The probability for a particle to select a tube at the entrance or inside the network was chosen to be proportional to the flow rate in that tube. Therefore, the motion of a particle was biased by the flow field in favor of the tubes that carried a larger flux of the fluid. This assumption, which is called “flow induced probability,” has been supported by experimental observation²⁰ and has been used in previous numerical network simulations (see, for instance, the review of Sahimi *et al.*⁸). Another important assumption that has been already mentioned in the last section was the perfect mixing at each node. This assumption dictated that the choice for a particle to enter a tube was independent of the previously

selected tubes. This last hypothesis might not be entirely realistic since particles might follow specific paths inside the filter.

Using the conservation of the flow in a tube of radius r , the particle velocity could be approximated as $Q/\pi r^2$ in that tube. The particle velocity was determined by the pressure forces acting on the particle in the tube, i.e., the pressure due to Poiseuille flow, $\Delta P_p = 8\nu\rho_f(l-d)Q/\pi r^4$ and the pressure due to gravity, $\Delta P_g = \pm 4/3\pi(d/2)^3(\rho_p - \rho_f)g/\pi r^2$ (with a negative sign when flow and gravity were in the opposite direction). This last term needed to be multiplied by $\sqrt{2}/2$ in the case of a network inclined at an angle of 45° . Since the inertial, electrostatic, Brownian, and molecular forces were taken to be negligible in the experiments, they were not taken into account in the numerical simulation.

Three capture mechanisms were implemented in the model. Since “constriction sites” were found to determine primarily particle capture, they were modeled by pores whose radii were smaller than that of the particle. If the radius of the tube was larger than the radius of the particle ($r-d/2 \geq 10^{-9}$), the particle was not “geometrically” captured and the particle continued to propagate inside the filter. Otherwise ($r-d/2 < 10^{-9}$), the particle was “geometrically” captured and the entrance to the tube was blocked. After capture, the conductance of the blocked tube was modified and was multiplied by a factor α . Since it was shown experimentally that the filter was not saturated, this factor was chosen to be $\alpha=1$. This means that each particle was released from the network after capture. It was, however, shown that different values of α gave the same results and therefore that α was not a relevant parameter for the present study. A particle could also be captured in a “levitation site.” This very rare event occurred when the drag force was smaller than the gravity force (in the opposite direction of the flow). Modeling the “hydrodynamic capture” found in the experiments was far less obvious since it required the knowledge of the complex flow structure inside the nodes. The following simplest model was implemented. If a particle reached a node such that the flow rates in the tubes had the same value within a 1%, it had the probability p_h to be captured at that node. Because of a lack of information, an *ad hoc* probability was adopted, $p_h = 1 - \exp(-\theta^2)$. This probability increased with particle size, as suggested by experimental observations. It reproduces the experimental finding that very small particles were never captured.¹⁴

2. Packets of particles propagating in the network

Since it was observed experimentally that packets of particles did not spread over the entire first layer of the packing, packets of particles were injected numerically on the central upstream plane of the network corresponding to a third of the total plane. Moreover, since it was also observed that two particles never penetrated in the same pore at the same time, this finding was implemented in the numerical simulation: if two particles selected the same tube, they could not enter it at the same time, but one after the other. The second particle had then to wait for the first to leave the tube before entering it. If the first particle was captured, the second selected a new tube and then continued to propagate into the network. Per-

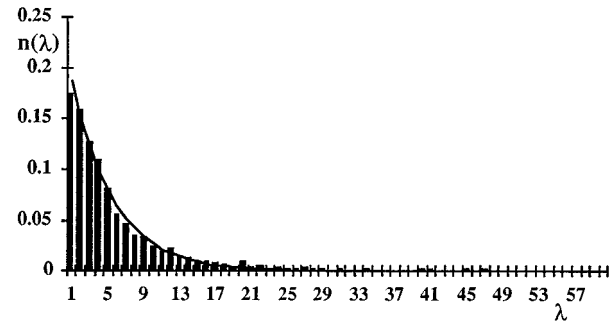


FIG. 5. Numerical results for the particle penetration depths for $\theta=0.160 \pm 0.01$ when particles were injected one by one with an upward flow.

fect mixing at each node was again assumed and the probability that a particle selected the next tube was again proportional to the flow rate in that tube.

The hydrodynamic interactions between particles inside a packet were also modeled. In addition to the pressure due to Poiseuille flow, ΔP_p , and the pressure due to gravity, ΔP_g , the extra pressure due to the presence of a particle in a tube, ΔP_+ , was also taken into account in modeling the propagation of particles. By applying the lubrication theory to the problem of the flow of a single particle in an isolated tube whose radius is close to that of the particle, this extra pressure was estimated as $\Delta P_+ = 4\nu\rho_f(Q/r^3) \times \sqrt{[d/(r-d/2)]}$. The particle velocity was again approximated as $Q/\pi r^2$ in the tube. Therefore, every time a particle entered a tube, the pressure drop in that tube was increased, and thereby the velocity field was changed within the network. When the particle left the tube, the tube recovered its previous conductance (unless it had become blocked) and the flow field was changed again within the network. When the packet of particles moves inside the network, the continuous entering of the particles in the tubes (or their plugging of the tubes) necessitates the continuous updating of the flow field. It should be mentioned that the relaxation time of the velocity field was assumed to be shorter than the time for particles to move through a tube, and so the velocity field was updated as soon as a particle left a tube. In addition to the three capture mechanisms described in the last section, the possibility of “relaunching” was also implemented. This phenomenon seemed indeed to play an important role in the propagation of packets deeper into the filter. A simple model was built to reproduce the “relaunching” of a captured particle by another particle passing by. A length characterizing the hydrodynamic interactions between particles, r^* , was introduced. Whenever a particle passed at a distance smaller than r^* from a captured particle, the captured particle could be released and selected another tube. Again, the flow field had to be continuously updated within the network.

V. NUMERICAL RESULTS AND COMPARISON WITH EXPERIMENTS

A. Particles injected one by one

Figure 5 presents the penetration depth distribution for 2000 particles injected one by one in the network. This nu-

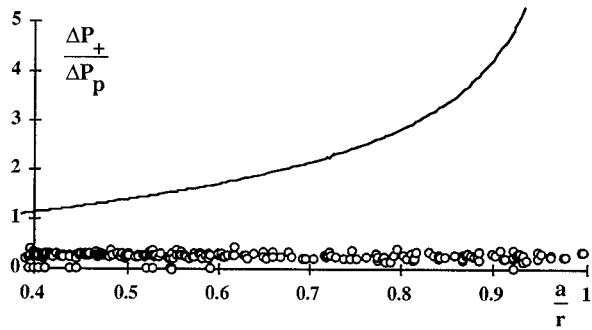


FIG. 6. Ratio between the extra-pressure in a tube due to a particle and the Poiseuille pressure drop (without a particle) for a tube in isolation (solid curve) and for a tube embedded in the network (empty circles).

merical result has been obtained for 250 network configurations. Only a total number of eight particles were injected inside each network in order to avoid saturation of the network. The particle size distribution was chosen to be a Gaussian distribution with a mean value $\theta=0.160$ and standard deviation 0.010 in order to model the experimental particle size distribution. The numerical distribution could be fitted by an exponential law as demonstrated by the χ^2 test. The characteristic length of the exponential decay was $\xi=4.7\pm 0.4$ and the median value of the distribution was $\lambda_m=6.0$. The predictions of the numerical simulation are found to be in good agreement with the experimental findings (Fig. 1) in the case of particles injected one by one. It should, however, be mentioned that the heterogeneity introduced at the entrance of the experimental packing induced smaller penetration depths at the entrance (see the first three bars of the histogram of Fig. 1). This was not observed in the numerical distribution (Fig. 5) because the entrance of the network did not have such an heterogeneity.

B. Particles injected by packets

In the numerical simulation, the ratio between the number of particles in a packet and the number of entrance tubes was set equal to 10% in order to mimic the experimental situation. The numerical results were obtained for 2000 particles injected by packets of 8 particles and for 250 network configurations. The particle size distribution was again chosen to be a Gaussian distribution with a mean value $\theta=0.160$ and standard deviation 0.010. Two main ingredients, i.e., the extra pressure due to the flow of a particle in a tube and the relaunching of a captured particle by another particle passing nearby, were present in the numerical simulation.

The first ingredient was not found to create a deeper penetration of packets of particles into the filter. Although the extra pressure along a tube was found to diverge as $d/2r \rightarrow 1$ for a tube in isolation, it remained of the order of 30% of the Poiseuille pressure drop (without a particle) for a tube embedded inside the network, as can be seen in Fig. 6. Indeed, when a particle entered a tube within the network, there were several other tubes that could carry the fluid away from this partially blocked tube.

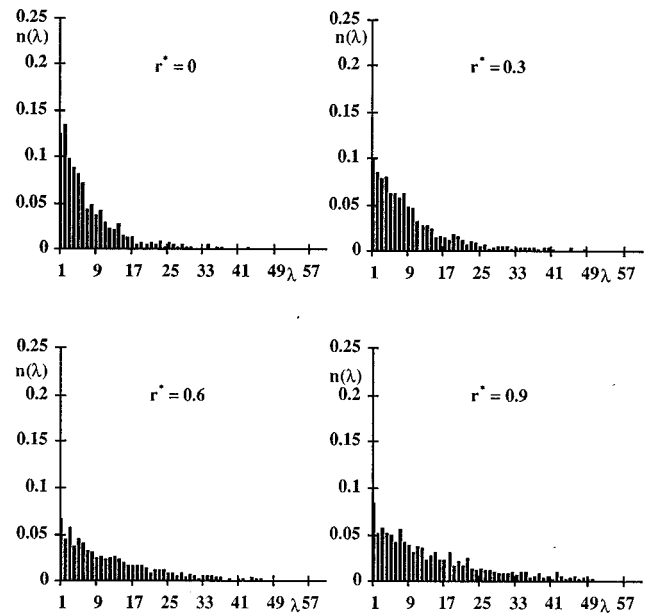


FIG. 7. Numerical results for the particle penetration depths for $\theta=0.160 \pm 0.01$ when particles were injected by packets with an upward flow for four different values of the interaction length $r^*=0, 0.3, 0.6,$ and 0.9 .

Conversely, the second ingredient was found to be determining in giving the “packet effect.” An estimation of the characteristic interaction length r^* was needed. This length was linked to the correlation length of the velocity fluctuations in the network, and it was estimated to be of the same order as the dispersion length of tracers in a porous medium.²¹ This length has been experimentally estimated as 0.6 times the size of the grain of the packing.²² This dispersion length was also found to depend upon the disorder of the medium.²³ Figure 7 shows the penetration depth distributions for $r^*=0, 0.3, 0.6,$ and 0.9 . As mentioned above, for $r^*=0$ the distribution was found to be similar to that of Fig. 5 and no significant change was observed. As soon as $r^*=0.3$, the particles penetrated deeper into the medium. For $r^*=0.6$ and $r^*=0.9$, the distributions were found to be in good agreement with the experimental distribution of Fig. 2. It is worth noting that the present unit length is the sphere diameter that corresponds to the size of the grain of the porous medium.

VI. CONCLUSIONS

In this study, some aspects of deep bed filtration have been visually and statistically studied for small non-Brownian particles flowing into a random packing of mono-size glass spheres at low Reynolds number. The particle transport was found to be convective in nature and steric effects and hydrodynamic and gravity forces were found to be dominant. The penetration depth distributions were examined for different particle injection methods, i.e., individually or in packets. It was discovered that packets of particles penetrated further than the same number of particles released one at a time. However, when the experiments were repeated without any flow across the medium, the penetration depth

distributions were found to be similar for both types of injection methods. These findings suggested that the collective effects observed when the particles were injected in packets were due to hydrodynamic phenomena. Moreover, investigation of the mechanisms of the particle capture by examining the stability of the capture sites revealed that the capture sites were not only constriction sites but also “hydrodynamic” sites, where particles could be released by local flow variations. In particular, a particle captured in an “hydrodynamic” site could be relaunched by another particle passing nearby.

A Monte Carlo simulation that approximated the packing by a two-dimensional square network of cylindrical tubes was developed jointly with the experimental study. The flow rate of the viscous fluid in the tubes was assumed to obey Poiseuille’s law with perfect mixing at the junctions between the tubes. Direct comparison with experiments allowed one to test the validity of the various basic ingredients introduced in the numerical model. The rules for junction motion were that a particle selected a new tube with a probability proportional to the fluid flux in the tube (“flow induced probability”), that if it came across a tube smaller than its diameter then its path was blocked, and that if it reached a junction such that the flow rates in the tubes had the same value within 1% it had a probability p_h of being captured. The first rule assumes that the motion of a particle is biased by the flow field in favor of the tubes that carry larger flux of the fluid. The second rule models constriction sites while the third rule is an attempt to take into account “hydrodynamic” capture sites. These ingredients were found to provide a realistic description of particle penetration depths when the particle propagated independently in the packing. Modeling the propagation of packets of particles required the implementation of additional ingredients in the simulation. Taking into account the additional pressure drop in a tube due to a particle was found not to be sufficient to reproduce the deeper penetration of packets of particles into the filter. A simple model was then built to reproduce the “relaunching” of a captured particle by another particle by introducing a length characterizing the hydrodynamic interactions between particles inside the filter. This last ingredient was found to be essential in predicting the collective effects when particles were injected by packets.

The key findings of this study reveal the deepening complexity of the phenomena that determine the penetration depths of the particles when hydrodynamic and gravitational forces are considered. The geometric structure is no longer the only consideration. It is necessary to take into account the interactions between the particles and the complex flow structure within the packing as well as the particle–particle interactions as soon as particles are not propagating alone inside the filter.

ACKNOWLEDGMENTS

This work is part of the thesis of C. Ghidaglia sponsored by the Centre de Recherches de Voreppe (Pechiney) and by the Centre National de la Recherche Scientifique. It was also undertaken under the auspices of the Groupement de Recher-

che du CNRS “Physique des Milieux Hétérogènes Complexes” and a NATO Collaborative Research Grant on “Particle Mixing by Percolation.” We wish to thank G. M. Homsy and J. Koplik for discussions. We would also like to thank F. Latrémolière, M. Nicolas, L. Oger, I. Raynal, and S. Tomlin for valuable help and O. Brouard, J.-C. Guibert, M. Mayeux, R. Porchet, and D. Vallet for technical assistance. We also thank F. Lacour for help in coating the acrylic beads. The Santicizer 160 was donated by Monsanto and the acrylic beads were supplied by du Pont de Nemours and Orkem Norsolor.

- ¹C. Tien, *Granular Filtration of Aerosols and Hydrosols* (Butterworths, Boston, 1989).
- ²J. P. Herzig, D. M. Leclerc, and P. LeGoff, “Flow of suspensions through porous media—Application to deep bed filtration,” *Ind. Eng. Chem.* **62**, 8 (1970).
- ³C. Tien and A. C. Payatakes, “Advance in deep bed filtration,” *AICHE J.* **25**, 737 (1979).
- ⁴J. Dodds, G. Baluais, and D. Leclerc, “Filtration processes,” in *Disorder and Mixing*, edited by E. Guyon, J.-P. Nadal, and Y. Pomeau (Kluwer Academic, Dordrecht, 1988), p. 163.
- ⁵D. Houi, “Filtration and porous media,” in *Hydrodynamics of Dispersed Media*, edited by J.-P. Hulin, A.-M. Cazabat, and E. Carmona (Elsevier, New York, 1990), p. 155.
- ⁶O. Lamrous, D. Houi, C. Zarccone, and J. Pradere, “Magnetic resonance imaging application to study porous media,” *Rev. Phys. Appl.* **24**, 607 (1989).
- ⁷A. R. Yevseyev, V. E. Nakoryakov, and N. N. Romanov, “Experimental investigation of a turbulent filtrational flow,” *Int. J. Multiphase Flow* **17**, 103 (1990).
- ⁸M. Sahimi, G. R. Gavalas, and T. T. Tsotsis, “Statistical and continuum models of fluid–solid reactions in porous media,” *Chem. Eng. Sci.* **45**, 1443 (1990).
- ⁹M. Leitzement, P. Maj, J. A. Dodds, and J. L. Greffe, “Deep bed filtration in a network of random tubes,” Chap. 19 of *Solid Liquid Separation*, edited by J. Gregory, published for the Society of Chemical Industry (Ellis Horwood, Chichester, 1984), p. 273.
- ¹⁰M. M. Sharma and Y. C. Yortsos, “A network model for deep bed filtration processes,” *AICHE J.* **33**, 1644 (1987).
- ¹¹A. O. Imdakm and M. Sahimi, “Transport of large particles in flow through porous media,” *Phys. Rev. A* **B6**, 5304 (1987).
- ¹²S. D. Rege and H. S. Fogler, “A network model for deep bed filtration of solid particles and emulsion drops,” *AICHE J.* **34**, 1761 (1988).
- ¹³C. Ghidaglia, E. Guazzelli, and L. Oger, “Particle penetration depth distribution in deep bed filtration,” *J. Phys. D* **24**, 2111 (1991).
- ¹⁴C. Ghidaglia, L. de Arcangelis, E. J. Hinch, and E. Guazzelli, “Particle capture transition in deep-bed filtration,” in preparation.
- ¹⁵D. Bideau, J.-P. Troadec, and L. Oger, “Désordre dans les empilements compacts de disques durs identiques,” *C. R. Acad. Sci. Paris* **297**, 219 (1983).
- ¹⁶J. A. Dodds, “The porosity and contact points in multicomponent random sphere packings calculated by simple statistical geometric model,” *J. Colloid Interface Sci.* **77**, 317 (1980).
- ¹⁷P. Meakin and R. Julien, “Simulation of small particle penetration in a random medium,” *J. Phys. France* **51**, 2673 (1990).
- ¹⁸G. Mason, “A model of the pore space in a random packing of equal spheres,” *J. Colloid Interface Sci.* **35**, 279 (1971).
- ¹⁹H. J. Frost, “Cavities in dense random packings,” *Acta Metall.* **30**, 889 (1982).
- ²⁰D. Houi, C. Zarccone, and P. Schmitz, “Visualizations of microfiltration processes,” *Proceedings of the 5th World Filtration Congress*, Nice, France, 1990.
- ²¹J. F. Brady and D. L. Koch, “Dispersion in porous media,” in Ref. 4, p. 107.
- ²²J. J. Fried and M. A. Combarnous, “Dispersion in porous media,” *Adv. Hydrosci.* **7**, 169 (1971).
- ²³J. Koplik, “Hydrodynamical dispersion in random network,” in Ref. 4, p. 123.